Multi-coupled Resonant Splitting with a Nano-slot Metasurface and PMMA Phonons

Michael F. Finch, Brian A. Lail
Department of Electrical and Computer Engineering, Florida Institute of Technology
150 West University Blvd., Melbourne, FL USA 32901

ABSTRACT

Coupled-resonances can be used in applications that include, but are not limited to, surface-enhanced infrared spectroscopy (SEIRS), surface-enhanced Raman spectroscopy (SERS), biosensing, and index sensing. Fano resonance in analogue plasmonic systems has been described as the coupling of a bright (superradiant) mode and a dark (subradiant) mode via the near field.Dark and bright mode interactionsareinvestigated with the use of a Fano resonant metamaterial (FRMM) where the metamaterial is a dual nano-slot metasurface on a silicon cavity. The FRMM is numerically simulated using Ansys High Frequency Structure Simulator (HFSS). The FRMM is coupled to the carbon double bond in polymethyl methacrylate (PMMA) to demonstrate mode splitting and signal enhancement. Then the dual nano-slot is compared to the complementary dual nano-rod configuration.

Keywords: normal mode splitting, multi-coupled resonant splitting, nano-slot metasurface, surface-enhanced infrared spectroscopy (SEIRS), Fano resonance, polymethyl methacrylate (PMMA), biosensing

1. INTRODUCTION

Optical and infrared (IR) metamaterials have produced exotic material properties through the use of pattering and layering of different materials[1] which gives rise to unique applications like cloaking[2], unique negative index optical devices[3], and sensing devices[4]. A metasurface is a subset of metamaterial in which only a patterned planar surface[5] which is advantageous for top-down fabrication methods. An application of particular interest for metasurface (or metamaterials) is in biosensing and ultasensitive surface enhanced vibrational spectroscopy in mid-infrared (MIR) like surface enhanced infrared spectroscopy (SEIRS) and surface enhanced Raman spectroscopy (SERS)[4,6-9].Fano introduced an asymmetric line shape resonance that now bears his name in his 1961 paper[10]. The Fano line shape is a result from coherent interference between broad and narrow resonances. The scattering cross section for Fano resonance (eq. 1) is typically used to describe the reflection or transmission[10-12]:

$$\sigma = \frac{(q+\epsilon)^2}{1+\epsilon^2} \tag{1}$$

where$\epsilon = (E-E_r)/\gamma$ is the reduced energy ($E_r$is a resonance's center value and full width half maximum of the resonance is related to γ) and q which describes coupling. A Fano resonant metamaterial (FRMM) is a metamaterial which exhibits Fano resonance evidence by the scattering cross section in the transmission or reflection coefficients.

This paper investigates the use of a FRMM and resonant coupling with an analyte material, Polymethyl methacrylate (PMMA), at the carbon oxygen double bond(C=O) vibrational resonance at 52 THz (1733 cm^{-1}). Resonant coupling has applications in biosensing and SEIRS. First, a FRMM structure with a dual nanoslot array and dual nanorod, Figure 2, will be designed using ANSYS HFSS[13]. Then an PMMA overlay will be placed on top of the metasurface the resonance coupling signature will be observed[7,14,15].

2. FANO RESONANT METAMATERIAL

The Fano resonant asymmetric line shape can be observed in the reflection and transmission. Temporal coupled mode theory (TCMT) has been used as a standard approach in a classical approximation of Fano resonance. A block diagram for TCMT is shown in Figure 1. In a TCMT description a bright mode (ω_B-jγ_B) is coupled to a dark mode (ω_D-jγ_D) via the near field with coupling strength "V"[11]. A coupled system of differential equations (eq. 2) can be described[11,16-18].

Plasmonics: Metallic Nanostructures and Their Optical Properties XIII, edited by Allan D. Boardman, Din Ping Tsai,
Proc. of SPIE Vol. 9547, 954710 · © 2015 SPIE · CCC code: 0277-786X/15/$18 · doi: 10.1117/12.2188644

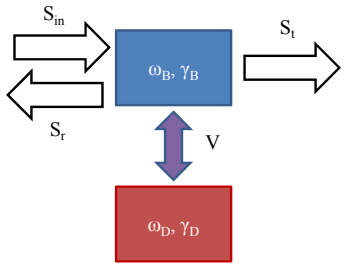

Figure 1. TCMT block diagram from Fano resonance with a bright-dark mode description.

$$\frac{da_B}{dt} - j(\omega_B + j\gamma_B)a_B + jVa_D = \alpha_B S^{in} e^{-j\omega t}$$
$$\frac{da_D}{dt} - j(\omega_D + j\gamma_D)a_D + jVa_B = \alpha_D S^{in} e^{-j\omega t} \quad (2)$$

In eq. 2, a_n are field amplitudes for the bright or dark mode, α_n describes how well the resonant modes couple to the incoming impending excitation (S^{in}). The bright mode will be defined as a low Q factor resonance that couples well to the excitation. Conversely, the dark mode will be a high Q factor resonances that couples weakly to the incoming radiation, and thus $\alpha_D \approx 0$[11,19]. Therefore assume time harmonic excitation at normal incidence, eq. 2 can be uncoupled into:

$$\frac{a_B}{s^{in}} = \frac{-j\alpha_B(\omega-\omega_D-j\gamma_D)}{(\omega-\omega_B-j\gamma_B)((\omega-\omega_D-j\gamma_D))-V^2}$$
$$\frac{a_D}{s^{in}} = \frac{-\alpha_B V}{(\omega-\omega_B-j\gamma_B)((\omega-\omega_D-j\gamma_D))-V^2} \quad (3)$$

The ratio a_B/S^{in} is typically consider to approximate to the Fano line shape[6], and will be used as a point for validating the simulated FRMM structures. ANSYS HFSS was used in modeling a metamaterial unit cells as seen in Figure 2. Ellipsometric-obtained measured data was imported into the model for increased accuracy for the gold and PMMA[20]. A gold metasurface was overlaid onto a silicon (Si) optical cavity suspended in air.

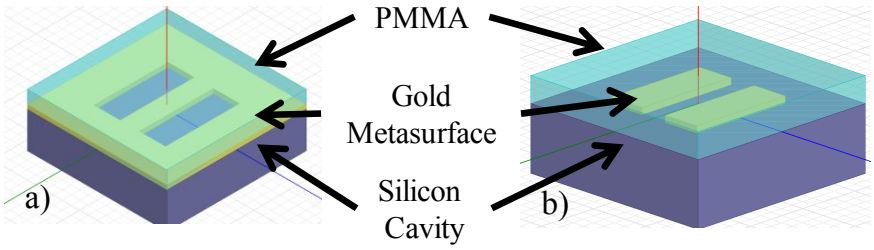

Figure 2. a) A unit cell of a FRMM consists of a dual nanoslotmetasurface of ellipsometric measured[20] gold optical properties on top of a silicon cavity. The resonant coupling structure consisted of a PMMA overlay on top of the FRMM. b) Similarly, the complementary unit cell FRMM metasurface (dual nanorod) is shown.

FRMM Nanoslot&Nanorod Results

The transmission coefficients for both the nanoslot and nanorod cases were designed to have the destined Fano resonant line shape which is seen in Figures 3a and 4a, respectively. A bright mode, as seen in Figure 3b-d or Figure 4b-d, will be defined to have parallel phase in H field (E field) along the slots(rods); conversely a dark mode will have anti-parallel phase in H field (E field) along the slots (rods)[21,22]. The TCMT mode does not take into consideration loss in metallization, therefore discrepancies in the mathematical relation compared to the simulated results can be observed in Figure 3e and 4e. The dark mode of the FRMM is strategically designed such that the null and dark mode is around the PMMA's phonon resonance. The dark mode's near field would then couple to phonon virbration mode to result in mode splitting.

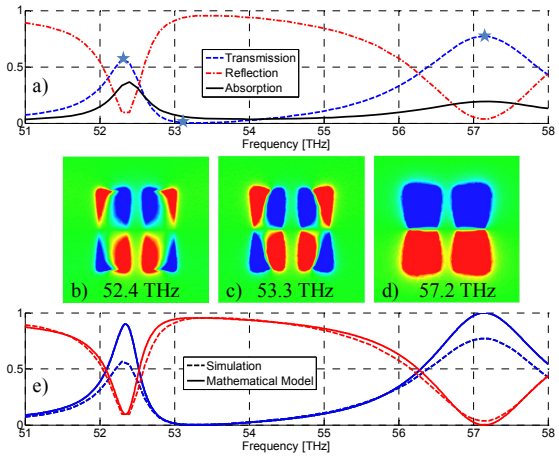

Figure 3. a) Simulated transmission, reflection, and absorption coefficients for a nanoslot FRMM. Dark quadpoles b) and c) are shown interacts with a bright dipole d) to result in a Fano resonant line shape. e) Transmission and reflection coefficients are parametrically fitted with the TCMT eq. 2 and eq. 3.

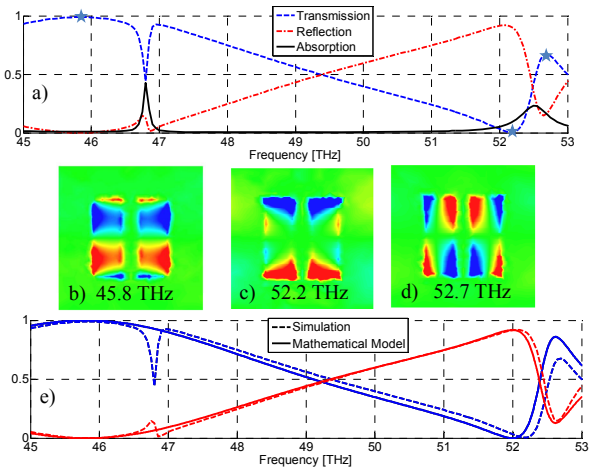

Figure 4. a) Simulated transmission, reflection, and absorption coefficients for a nanorod FRMM similar to Figure 3 is shown for comparison. A bright quadpole b) is shown to interact with dark quadpoles c) and d) to result in a Fano resonant line shape. e) Transmission and reflection coefficients are parametrically fitted with the TCMT eq. 2 and eq. 3.

3. RESONANT COUPLING FRMM RESULTS

The resonant coupling results in mode splitting which is described with anti-crossing dispersion diagrams[14,15,23-25].With the introduction of additional modes, the TCMT description used to describe Fano resonance can be expanded and using a matrix notation the TCMT in the case of multi-resonance systems can be generalized to[23,26]:

$$\frac{d}{dt}\begin{bmatrix} a_1 \\ a_2 \\ \vdots \\ a_n \end{bmatrix} = -j\begin{bmatrix} \omega_1 & V_{12} & \cdots & V_{1n} \\ V_{21} & \omega_2 & & \\ \vdots & & \ddots & \\ V_{n1} & & & \omega_n \end{bmatrix}\begin{bmatrix} a_1 \\ a_2 \\ \vdots \\ a_n \end{bmatrix} \tag{4}$$

Using numerical methods, it can be seen in Figure 5 for both nanoslot (top) and nanorod (bottom) that there is mode splitting signature in the reflection coefficient as a result of the interaction with the PMMA compare to Figures 3a and 4a there is splitting at around 52 THz.

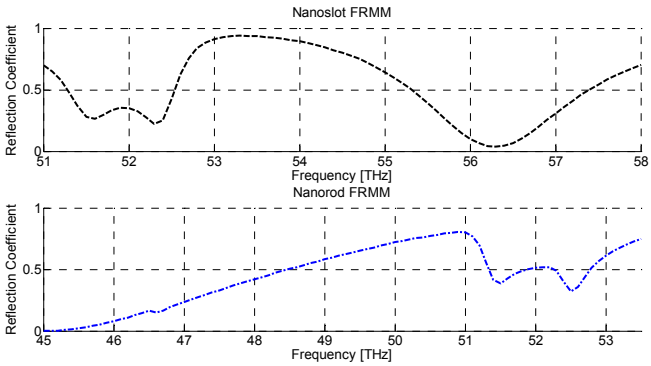

Figure 5. The resonant coupling signature at 52 THz is observed in both the case of the nanoslot (top) and nanorod (bottom).

Asymmetrical FRMM (AFRMM): Nanoslot&Nanorod Results

Asymmetry in the nanoslot and nanorod (Figure 6) was parametrically swept numerically and the results are shown in Figure 7 where $\alpha = (1-\Delta L/L)*100\%$. From Figure 7 left, it can be seen that tuning the asymmetry in the metasurfaces results in enhancement in the coupled resonance response. Where enhancement is defined as a reduction in reflection thus increase in absorption and transmission. The tuning of asymmetry in FRMM in Figure 7 is similar to what has been reported[6,27].

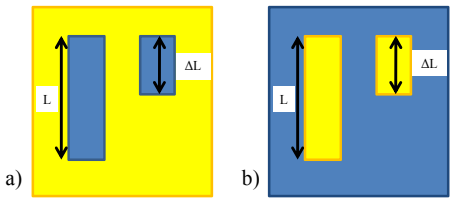

Figure 6. The asymmetry of the nanoslot (a) and nanorod (b) metasurface to produce an AFRMM is shown.

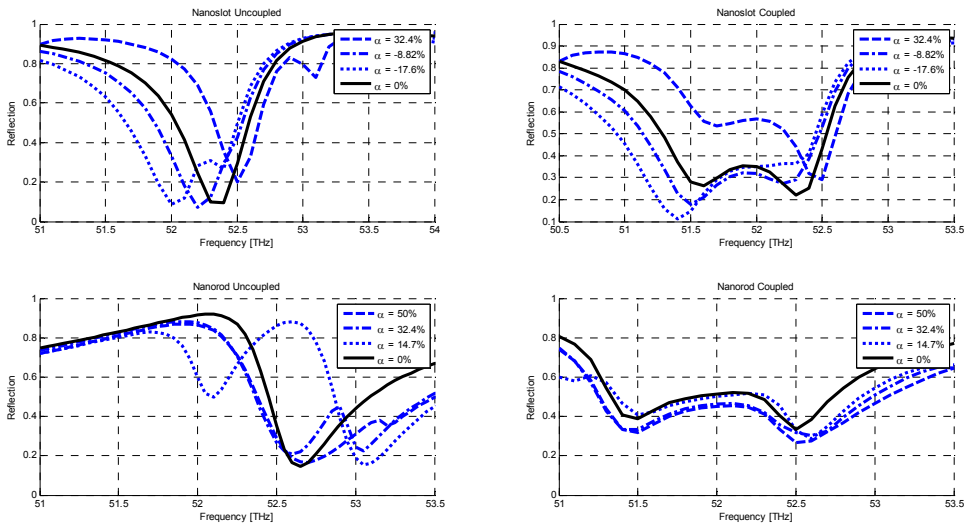

Figure 7. AFRMM nanoslot (top left) and nanorod (bottom left) multi-mode tuning due to asymmetry in the metasurface. Resonant coupling of PMMA with nanoslot (top right) and nanorod (bottom right) is observed. Asymmetric multi-resonant tuning is shown to result in enhancement of the reflected signal.

4. CONCLUSION

In both cases in Figures 3a and 4a, the nanoslot and nanorod Fano resonance line shape was considered to be related to the transmission coefficient. However, with the use of Babinet's principle and by considering complementary metasurfaces, the transmission and reflections coefficients in a lossless case would swap[16,28-30]. Therefore, in the complementary case to Figure 3a and 4a, the reflection coefficient would have the Fano resonant line shape. If an electromagnetically induced transparency (EIT) or absorption (EIA) description was used for resonant coupling, then the mode splitting signature would be present (similar to Figure 7, right). However; rather than having an EIA coupled system, evident from the transmission coefficient, an EIT system would be present resulting from the nature of complementary metasurface EIT/EIA pairing[30]. A device was designed with a simple nanoslot or nanorod array metasurface with the transmission coefficient exhibiting asymmetrical Fano resonant line shape thus resulting in a FRMM. Then an AFRMM was investigated, via breaking the metasurface symmetry, resulting in multi-resonant tuning which leads to an enhancement of the resonant coupling signature as shown in Figure 7. Devices employing AFRMM can help pave the way for advancement in sensitivity for IR vibration spectroscopy applications.

REFERENCES

[1] Balanis, C. A., [Advanced Engineering Electromagnetics], 2nd ed. Hoboken, NJ: John Wiley & Sons, Inc., (2012).

[2] Schurig, D., et al., "Metamaterial electromagnetic cloak at microwave frequencies," Science 314(977), 977-980 (2006).

[3] Pendry, J. B., "Negative refraction makes a perfect lens," Physical Review Letters 85(18), 3966-3969 (2000).

[4] Chen, T., Li, S., and Sun, H., "Metamaterials Application in Sensing," Sensors 12(3), 2742-2765 (2012).

[5] Kildishev, A. V., Boltasseva, A., and Shalaev, V. M., "Planar Photonics with Metasurfaces," Science 339(6125), 1232009-1 - 1232009-6 (2013).

[6] Wu, C., et al., "Fano-resonant asymmetric metamaterials for ultrasensitive spectroscopy and identification of molecular monolayers," Nature Materials 11, 69-75 (2012).

[7] Chen, K., Adato, R., and Altug, H., "Dual-Band Perfect Absorber for Multispectral Plasmon-Enhanced Infrared Spectroscopy," ACS Nano 6(9), 7998-8006 (2012).

[8] Adato, R., Aksu, S., and Altug, H., "Engineering mid-infrared nanoantennas for surface enhanced infrared absorption spectroscopy," Materials Today 00(00), 1-11 (2015).

[9] Alici, K. B.,"Hybridization of Fano and vibrational resonances in surface-enhanced infrared absorption spectroscopy of streptavidin monolayers on metamaterial substrates," IEEE Transactions on Nanotechnology 13(2), 216-221 (2014).

[10] Fano, U., "Effects of Configuration Interaction on Intensities and Phase Shifts," Physical Review 124(6), 1866-1878 (1961).

[11] Khanikaev, A. B., Wu, C., and Shvets, G., "Fano-resonant metamaterials and their applications," Nanophotonics 2(4), 247-264 (2013).

[12] Rau, A. R. P., "Perspectives on the Fano resonance formula," Physica Scripta 69(1), C10-C13 (2004).

[13] Ansoft Corporation, [An Introduction To HFSS: Fundamental Principles, Concepts, and Use]. Pittsburgh, PA: Ansoft, LLC, (2009).

[14] Finch, M. F., and Lail, B. A., "Modeling of resonant coupling between infrared nanowire metasurface and phonons in PMMA," in The 30Th Annual Review of Progress in Applied Computational Electromagnetics, Computational Methods in Nanoelectromagnetics, Jacksonville (2014).

[15] Finch, M. F., and Lail, B. A., "Mode splitting and resonant coupling between a slot metasurface and PMMA," in Proc. SPIE 9202, Photonic Applications for Aerospace, Commercial, and Harsh Environments V, San Diego (2014).

[16] Verlegers, L., Yu., Z., Ruan, Z., Catrysse, P. B., and Fan, S., "From electromagnetically induced transparency to superscattering with a single structure: a coupled-mode theory for doubly resonant structures," Physical Review Letters 108(8), 083902: 1-5 (2012).

[17] Haus, H. A., and Huang, W., "Coupled-Mode Theory," Proceeding of the IEEE 79(10), 1505-1518 (1991).

[18] Lovera, A., Gallinet, B., Nordlander, P., and Martin, O. J. F., "Mechanisms of Fano Resonances in Coupled Plasmonic Systems," ACS Nano 7(5), 4527-4536 (2013).

[19] Wan, W., Zheng, W., Chen, Y., and Liu, Z., "From Fano-like interference to scuperscattering with a single metallic nanodisk," Nanoscale 6(15), 9093-9102 (2014).

[20] Ginn, J. et al., "Characterizing Infrared Frequency Selective Surfaces on Dispersive Media," ACES Journal 22(1), 184-188 (2007).

[21] Ding, J. et al., "Tuneable complementary metamaterial structures bases on graphene for single and multiple transparency windows," Scientic Reports 4(6128), 1-7 (2014).

[22] Omaghali, N. E. J., Tkachenko, V., Andreone, A., and Abbate, G., "The optical Fano resonance in asymmetric dimer metamaterial," in Proc. SPIE 8423, Metamaterials VII, 842304, Brussels, Belgium , 842304-1:7 (2012).

[23] Shelton, D., "Tunable Infrared Metamaterials," University of Central Florida, Orlando, FL, PhD Dissertation CFE0003201, (2010).

[24] Finch, M. F., and Lail, B. A., "Normal mode splitting with lossy coupled resonances," in The 31Th Annual Review of Progress in Applied Computational Electromagnetics, Williamsburg (2015).

[25] Neubrech, F., Weber, D., Ender, D., Nagao, T., and Pucci, A., "Antenna sensing of surace phonon polaritons," Journal of Physical Chemistry C 114(16), 7299-7301 (2010).

[26] Zhang, X., et al., "Electromagnetically induced absorption in a three-resonator metasurface system," Scientific Reports 5(10737), 1-9 (2015).

[27] Singh, R., et al., "The Fano resonance in symmetry broken terahertz metamaterials," IEEE Transactions on terahartz science and technology 3(6), 820-826 (2013).

[28] Falcone F., et al., "Babinet principle applied to design of metasurfaces and metamaterials," Physical Review Letters 93(19), 197401: 1-4 (2004).

[29] Al-Naib, I. A. I., Jansen, C., and Koch, M., "Applying the Babinet principle to asymmetric resonators," Electronics Letters 44(21), 1228-1229 (2008).

[30] Alyones, S., "Electromagnetically induced absorption in metamaterials in the infrared frequency," Progress in Electromagnetics Research Letters 47, 19-24 (2014).